A novel pre-sintering technique for the growth of Y–Ba–Cu–O superconducting single grains from raw metal oxides

2017 Supercond. Sci. Technol. 30 095001

(http://iopscience.iop.org/0953-2048/30/9/095001)

OPEN ACCESS

Made open access 8 August 2017

IOP Publishing

Superconductor Science and Technology

Supercond. Sci. Technol. **30** (2017) 095001 (9pp)

https://doi.org/10.1088/1361-6668/aa7999

A novel pre-sintering technique for the growth of Y–Ba–Cu–O superconducting single grains from raw metal oxides

Jiawei Li[1,2], Yun-Hua Shi[2], Anthony R Dennis[2], Devendra Kumar Namburi[2], John H Durrell[2], Wanmin Yang[1] and David A Cardwell[2]

[1] School of Physics and Information Technology, Shaanxi Normal University, Xi'an, Shaanxi 710119, People's Republic of China

[2] Department of Engineering, University of Cambridge, Trumpington Street, Cambridge CB2 1PZ, United Kingdom

E-mail: jwli@snnu.edu.cn

Received 1 April 2017, revised 29 May 2017
Accepted for publication 14 June 2017
Published 26 July 2017

Abstract

Most established top seeded melt growth (TSMG) processes of bulk, single grain Y–Ba–Cu–O (YBCO) superconductors are performed using a mixture of pre-reacted precursor powders. Here we report the successful growth of large, single grain YBCO samples by TSMG with good superconducting properties from a simple precursor composition consisting of a sintered mixture of the raw oxides. The elimination of the requirement to synthesize precursor powders in a separate process prior to melt processing has the potential to reduce significantly the cost of bulk superconductors, which is essential for their commercial exploitation. The growth morphology, microstructure, trapped magnetic field and critical current density, J_c, at different positions within the sample and maximum levitation force of the YBCO single grains fabricated by this process are reported. Measurements of the superconducting properties show that the trapped filed can reach 0.45 T and that a zero field J_c of 2.5×10^4 A cm^{-2} can be achieved in these samples. These values are comparable to those observed in samples fabricated using pre-reacted, high purity commercial oxide precursor powders. The experimental results are discussed and the possibility of further improving the melt process using raw oxides is outlined.

Keywords: bulk superconductor, YBCO single grains, top seeded melt growth, melt textured growth, raw oxides, sintering

(Some figures may appear in colour only in the online journal)

1. Introduction

(RE)–Ba–Cu–O [(RE)BCO] bulk high temperature superconductors (HTS), where RE is a rare-earth element or Y, have attracted considerable attention since the discovery of the YBCO system in 1987 [1]. Potential applications of bulk HTS include high-magnetic-field permanent magnets, magnetic bearings, magnetic separators and levitated transportation systems [2–5]. Over the past thirty years, therefore, there has been a concerted effort world-wide to develop these materials for practical applications [6–9]. The superconducting properties of the bulk (RE)BCO superconductors have improved significantly over this period due primarily to the development of melt processing techniques, such as top seeded infiltration growth (TSIG) or top seeded melt growth (TSMG) [10–15], to fabricate grain boundary-free, large, single grain superconductors. Indeed, these processes have led to the generation of a world record trapped field 17.6 T between a stack of two GdBCO bulk single grain samples at 26 K [7].

Both the TSMG and TSIG processes involve placing a structurally compatible seed crystal of similar lattice parameters

to the target superconducting $YBa_2Cu_3O_{7-\delta}$ (Y-123) phase on the top surface of a pressed powder pellet prior to melt processing. This assembly is then melt-processed at a temperature of around 1000 °C followed by slow cooling, during which, in a peritectic reaction nucleating at the seed, a non-superconducting Y_2BaCuO_5 (Y-211) phase reacts with liquid $Ba_3Cu_5O_8$ to form the desired superconducting RE-123 phase. In this way, a polycrystalline material is converted into a single grain (a so-called quasi-single crystal) with the superconducting matrix adopting the crystallographic orientation of the seed. To date, the synthesis of pure Y-123 and Y-211 phase powder has been an essential requirement for both the TSMG and TSIG techniques. The synthesis of pure phase precursor powder by solid-state reaction can take up to a week, however, which prolongs the fabrication process and leads to a low efficiency and high cost process. This additional processing limits further the batch production of YBCO bulk superconductors and its potential for commercially viable applications.

Reducing the number of steps in the fabrication of (RE)BCO precursor powders can effectively simplify the process flow and decrease the cost of the samples via a readily scalable production process. Three separate precursor powders (Y-211, Y-123 and $Ba_3Cu_5O_8$ or $BaCuO_2$) are usually required in a conventional TSIG process [16, 17], although Li *et al* [18] recently proposed a modified TSIG process based on the use of only two precursor powders (Y-211 and $BaCuO_2$). Yang *et al* [19, 20] further developed the modified TSIG process in which $BaCuO_2$ is the only required pre-reacted precursor powder. These studies indicate that pure phase Y-211 and Y-123 precursor powders are not essential to achieve a complete peritectic reaction and the subsequent growth of YBCO single grains in a seeded melt process, and that it is possible to use a mixture of raw oxides, from which Y-123 and Y-211 form via chemical reaction during melt processing, rather than pure Y-123 and Y-211 to fabricate large YBCO single grains. Y-123 single grains are formed via the same peritectic reaction between Y-211 and liquid $Ba_3Cu_5O_8$ in both TSMG and TSIG processes, despite the different liquid phase supply mechanisms that take place during the initial heating stage of the precursor arrangement at the beginning of each melt process. As a result, it is reasonable to assume that a mixture of raw oxides, most of which would react into Y-123 and Y-211 in both TSMG and TSIG, can be used as precursor powders in both processing techniques.

Meanwhile, the TSMG method is relatively economical, and significantly less complex, compared to the TSIG process, which requires two pressed precursor pellets. We propose a modified TSMG method for fabricating single grain YBCO bulk superconductors using a sintered mixture of Y_2O_3, BaO_2 and CuO as a precursor powder to avoid the time-consuming pre-synthesis of Y-123 and Y-211 precursors. The growth morphology, microstructure, levitation force and the trapped magnetic field of YBCO single grains fabricated using sintered raw mixed oxides have been investigated comprehensively, and the results compared with a standard YBCO single grain fabricated using commercial Y-123 and Y-211 precursor powders.

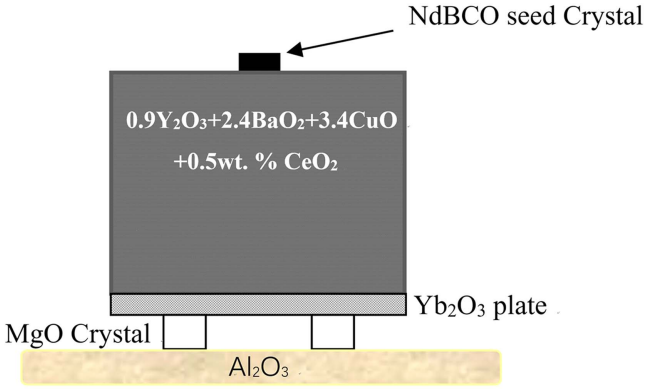

Figure 1. Arrangement of the samples for the TSMG process.

2. Experimental

Y_2O_3 (99.99%, Alfa Aesar), BaO_2 (95%, Sigma Aldrich), CuO (99.7%, Alfa Aesar) and CeO_2 (99.9% Sigma Aldrich) raw oxide powders were mixed in a composition ratio of $0.9Y_2O_3 + 2.4BaO_2 + 3.4CuO + 0.5\ wt\%CeO_2$ using an electric pestle and mortar to achieve a target composition of Y-123 + 0.4Y-211 + 0.5 wt%CeO_2 after chemical reaction at a high temperature. The sample was then sintered at 890 °C for 10 h in air, cooled to room temperature and ground to form the new precursor powder (NPP). Y-123 (99.9%, Adelwitz Technologiezentrum GmbH (ATZ), Y-211(99.9%, ATZ) and CeO_2 (99.9%, Sigma Aldrich) commercial powders were also mixed in a composition of Y-123 + 0.4Y-211 + 0.5 wt%CeO_2 using an electric pestle and mortar to form the conventional precursor powder (CPP) to enable the two precursor melt processes to be compared. The addition of CeO_2 is helpful to improve the superconducting properties of the single grain samples by refining the size of Y-211 particles [21].

The NPP was sintered and x-ray powder diffraction (XRD, SIEMENS Diffractometer D500) was used to examine the formation of the phases for both CPP and NPP. Differential thermal analysis (DTA, Setaram LabSys Evo) was performed to analyse phase changes and their equivalent temperatures for both precursor powders as a function of temperature.

Precursor powders of both NPP and CPP were pressed uniaxially into pellets of diameter 25 mm and mass 20 g. A well-textured NdBCO seed crystal, which is cut from a large NdBCO single grain fabricated by the Cambridge Bulk Superconductivity Group, was placed on at the centre of the top surface of each precursor pellet, which, in turn, was placed on a Yb_2O_3 support plate (diameter 25 mm, mass 3 g) in a cylindrically symmetric arrangement, as shown schematically in figure 1.

The melt process for both CPP and NPP compositions consisted of heating the sample to 930 °C at a rate of

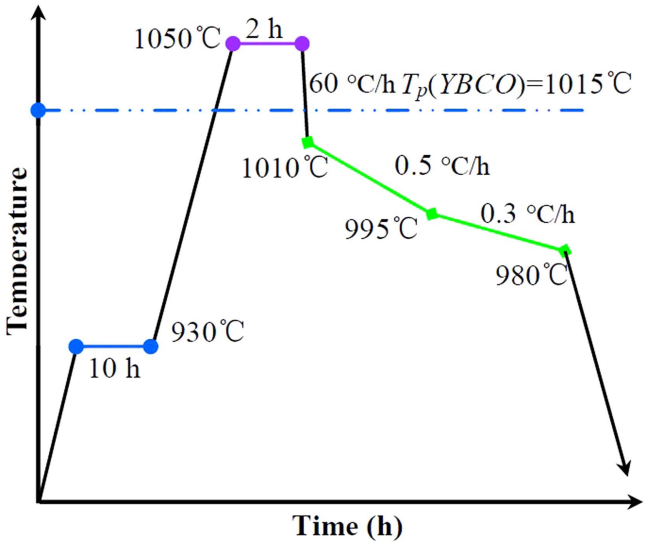

Figure 2. Heating profile for the growth of YBCO single grains.

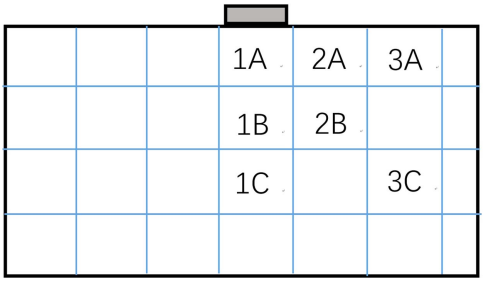

Figure 3. Schematic illustration of the positions of the specimens within a cross-section of the single grain for the measurement of T_c and J_c.

200 °C h^{-1}, holding at this temperature for 10 h, heating further to 1050 °C at a rate of 60 °C h^{-1}, holding for 2 h and cooling to 1010 °C at a rate of 60 °C h^{-1}. The samples were then cooled slowly to 995 °C at a rate of 0.5 °C h^{-1}, then cooled to 980 °C at a rate of 0.3 °C h^{-1} before, finally, furnace cooling to room temperature. The heating profile used was same for all the samples, as shown in figure 2. Following TSMG, the as-grown, single-domain YBCO samples were heated to 445 °C in a tube furnace and cooled slowly to 420 °C in flowing oxygen for 200 h. The samples fabricated with NPP and CPP were labelled as S1, S3 and S2, S4, respectively. The difference between samples S1, S2 and S3, S4 is that samples S3 and S4 were compacted using a cold isostatic press (CIP) at 2000 bar prior to melt processing.

The microstructures of the fully processed single grains were observed using a polarised light microscope (Nikon, model ECLIPSE ME600) and a scanning electron microscope (SEM, Hitachi TM3000). Image J software was used to analyze the size distribution of pores in the YBCO matrix. The levitation forces and trapped fields of the samples were measured at 77 K (the boiling point of liquid nitrogen). Subsequently, thin slabs were sliced from the centre of each single grain, which were cut further systematically into smaller specimens of approximate dimensions 1.5 × 2.0 × 1.0 mm^3, as shown in figure 3. The magnetic moments of these specimens were measured using a SQUID magnetometer (Quantum Design, model MPMS-XL). The superconducting critical temperatures (T_c) of the specimens were measured by cooling the samples to 80 K, applying a magnetic field of 0.002 T perpendicular to the *ab* plane of the single grain and measuring their magnetic moment as the temperature was increased from 80 to 92 K. The specimens were cooled to 77 K in zero applied field and their magnetization hysteresis loops measured under applied field from −6 to +6 T applied perpendicular to the *ab* plane of each sample. The extended Bean critical state model was then used to calculate J_c of each specimen from the width of the measured hysteresis loop [22].

3. Results and discussion

3.1. Surface morphology

Figure 4 shows photographs of the top surfaces of samples S1, S2, S3 and S4. It is evident that all the samples exhibit a characteristic single grain morphology, as indicated by epitaxial growth from the seed, the presence of quasi-facet growth lines on the top surface of the sample and the absence of the formation of spontaneous satellite grains towards the periphery of the sample. This demonstrates clearly that both NPP and CPP can be used to successfully fabricate single grains via the TSMG method. Because the synthesis of Y-123 and Y-211 is avoided and the cost of commercial Y_2O_3, CuO and BaO_2 oxides is less than one tenth of that of Y-123 or Y-211, this fabrication process of large, YBCO single grains represents a considerable saving in both time and cost.

3.2. Levitation force

A permanent magnet (20 mm in diameter, height 20 mm) with a central surface magnetic field of about 0.5 T was used for the levitation force measurements following zero-field cooling to 77 K. Figure 5 shows the measured levitation forces of samples S1 (NPP) and S2 (CPP) as a function of distance between the YBCO sample and the permanent magnet. The maximum levitation forces of samples S1 and S2 are 36 and 47 N, respectively, corresponding to a maximum levitation force densities of 11.46 and 14.96 N cm^{-2} (the diameter of both samples is 20 mm). The maximum levitation force density of the sample fabricated with the NPP is smaller than that of the sample fabricated with the CPP, although slightly higher than that observed for a YBCO sample fabricated by the TSIG technique, measured under the same experimental conditions, with optimum Bi_2O_3 doping, which is 10.82 N cm^{-2} [23]. These results indicate that the levitation performance of the samples fabricated in this study by both precursor power routes is comparable to that of other YBCO processing routes and that the use of a sintered mixture of

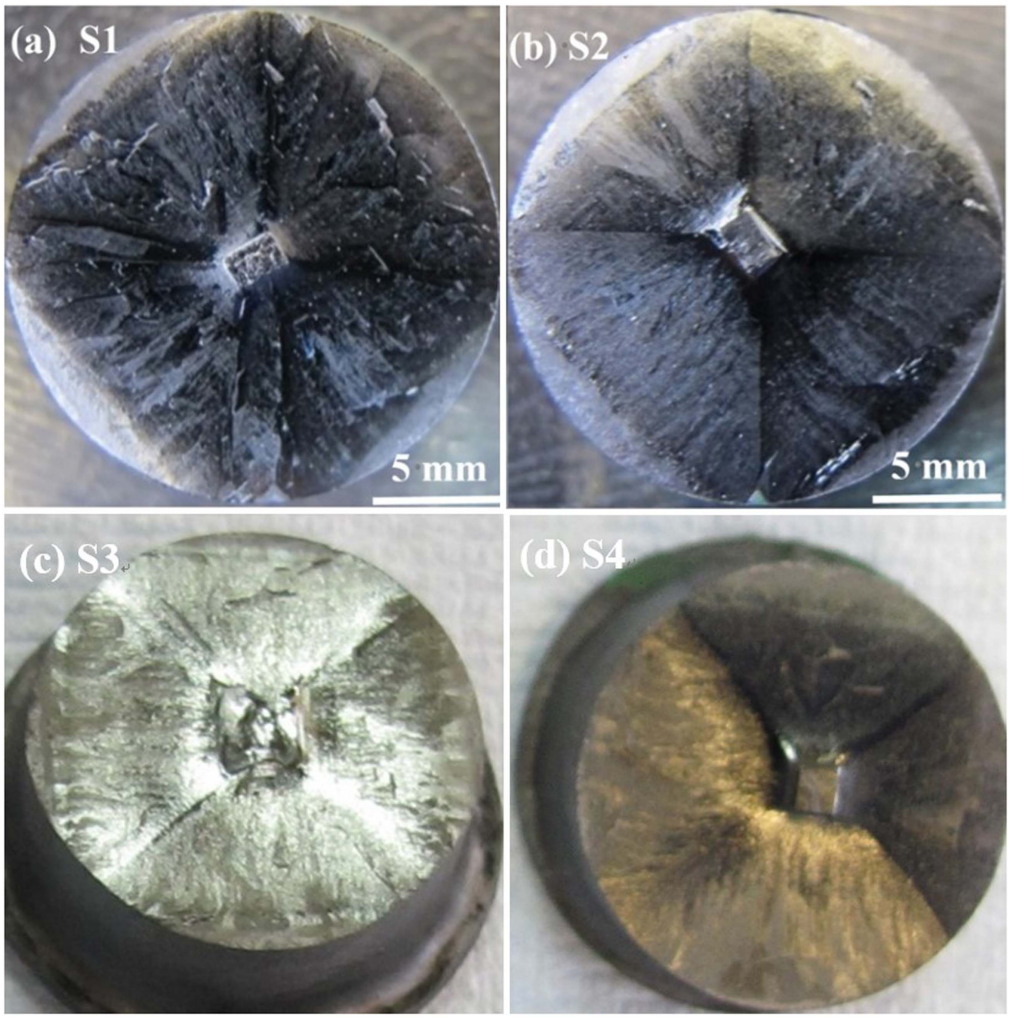

Figure 4. Top surface morphology of YBCO samples S1–S4 using (a) NPP, (b) CPP, (c) NPP pressed using CIP, and (d) CPP pressed using CIP.

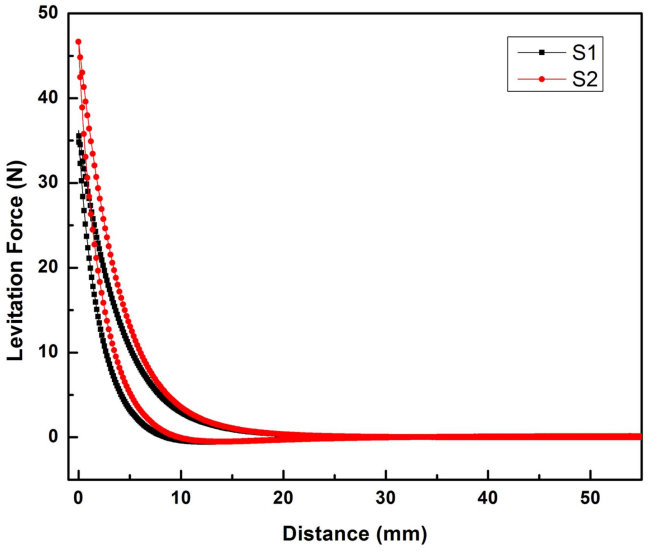

Figure 5. Levitation force as a function of distance for samples S1 (NPP) and S2 (CPP).

Y_2O_3, BaO_2 and CuO in the modified process, rather than a commercial precursor composed of mixed Y-123 and Y-211 pre-reacted phases, does not compromise significantly the levitation force properties of the bulk single grains.

3.3. Trapped magnetic field

The trapped fields of the samples were measured after a field cooling process (FC) in an applied field of 1.3 T. Figure 6 shows the distribution of the trapped magnetic flux density of all four samples S1, S2, S3 and S4, which have maximum trapped fields of 0.40 T, 0.44 T, 0.50 T and 0.56 T, respectively. For comparison, the average trapped field for YBCO single grains of diameter 20 mm reported by other authors is typically 0.5 T $\pm$ 0.1 T. The trapped fields of samples S1 and S3 (NPP) are not particularly high, although they do lie within the range of a standard sample. It can be seen that sample 1 has the lowest trapped field, although this is improved significantly, from 0.40 to 0.50 T by pressing the green body by

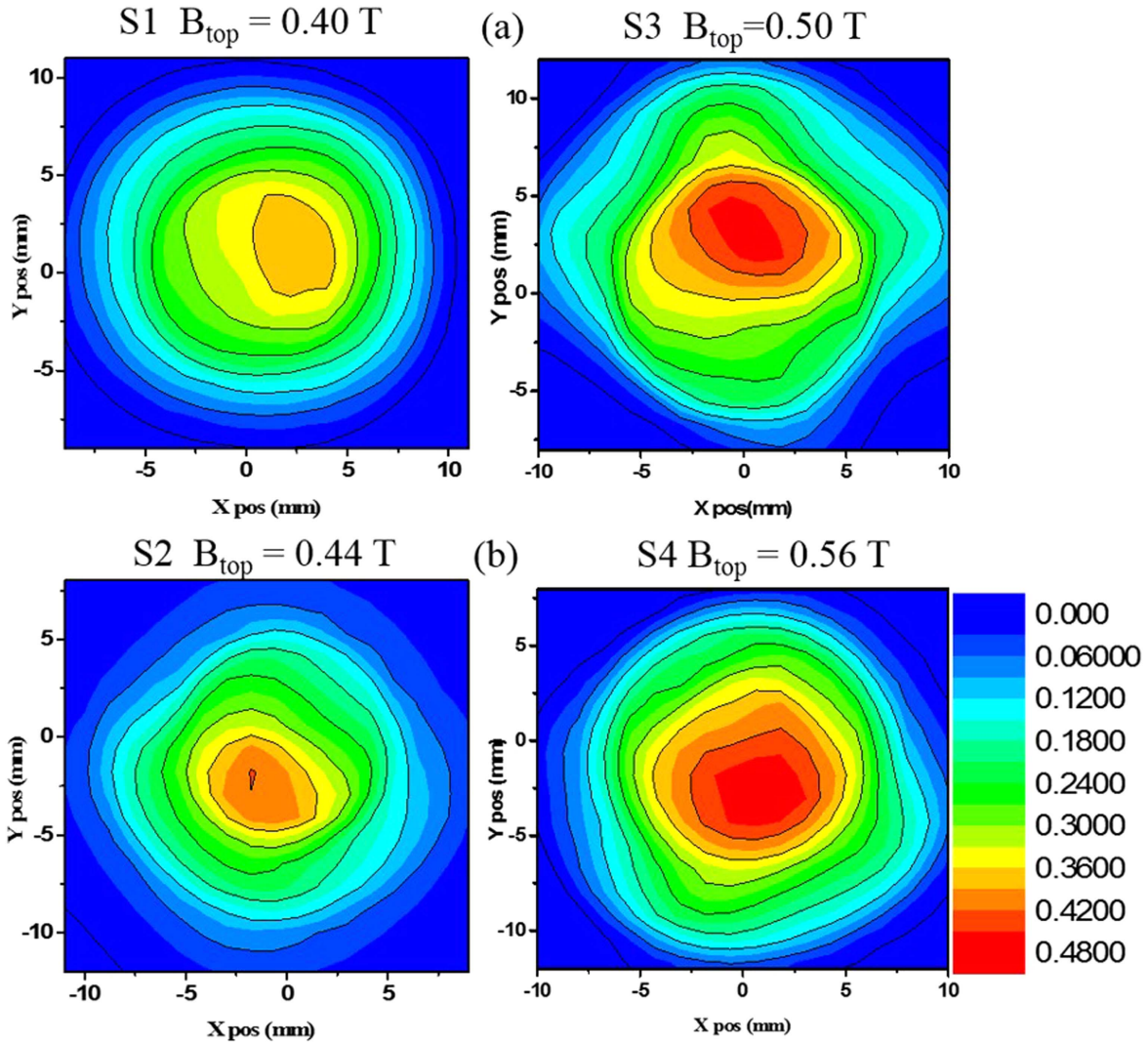

Figure 6. The distribution of the trapped field of YBCO samples S1–S4 prepared by the two precursor compositions (a) NPP and (b) CPP.

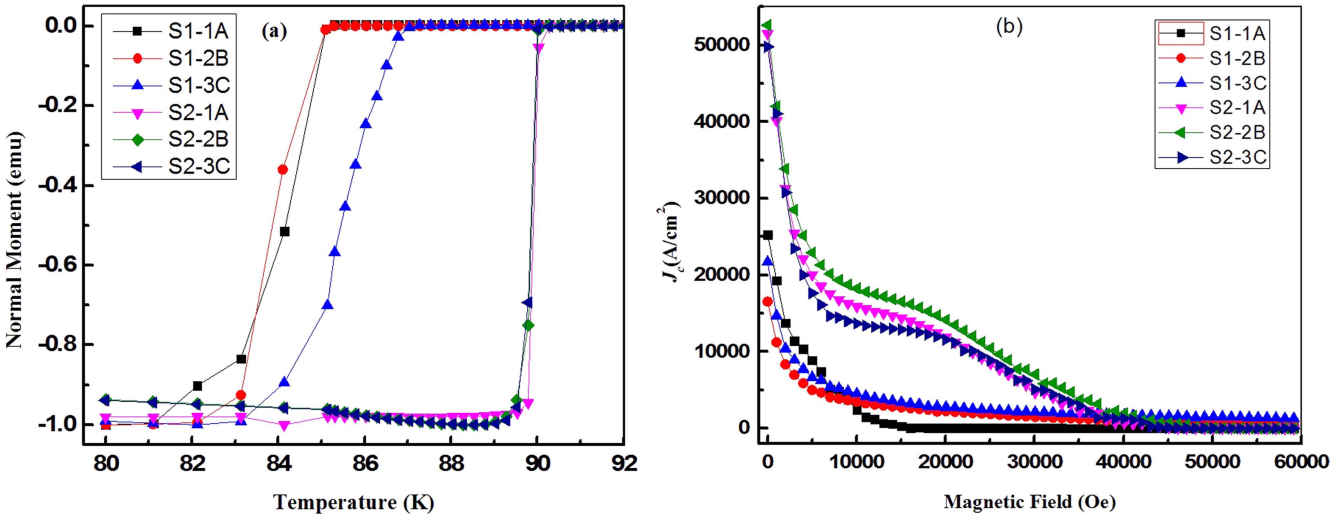

Figure 7. T_c and J_c of the specimens at different positions of YBCO samples S1 (NPP) and S2 (CPP).

CIP. A similar increase in maximum trapped field from 0.44 to 0.56 T was also observed for samples S2 and S4 (CPP) under otherwise identical measurement conditions. Therefore, it is clear that the growth of YBCO using raw sintered oxide precursor powders has achieved trapped fields that are comparable to those fabricated using commercial powders and are not significantly lower than the maximum field of 0.596 T, reported to date under similar measurement conditions [24].

3.4. Critical temperature T_c and critical current J_c

Figure 7 shows T_c and J_c of specimens at positions 1a, 2b and 3c of samples S1 and S2. It can be seen that the values of T_c for the sample S1 fabricated with the NPP are lower and broader than those of sample S2 (CPP). The three specimens fabricated by the CPP all exhibit the same T_c of 90 K and a sharp superconducting transition width. A similar trend is apparent in figure 7(b), with the values of $J_c(0)$ for sample S1 (NPP) varying from 1.7×10^4 to 2.6×10^4 A cm^{-2}, whereas higher $J_c(0)$ values of between 5.0×10^4 to 5.4×10^4 A cm^{-2} are observed for sample S2 (CPP). It is widely understood for YBCO that the onset T_c at different positions within the large single grain does not fluctuate greatly because the Y-123 superconducting phase is a uniformly stoichiometric compound. J_c varies with position, on the other hand, due to different concentrations of pinning centres at different positions within a single grain. The measurement of T_c at three positions of the sample made by the CPP show a consistent onset T_c and narrow ΔT, which indicates a uniform superconducting Y-123 phase presence at different positions in the single grain. However, in the sample prepared using the NPP, the onset T_c is observed to vary with position in the single grain and to exhibit a broad transition width, suggesting that the Y-123 phase may not be completely or correctly formed during the melt process. J_c at equivalent positions in the NPP single grain, therefore, may be low as a direct consequence of low local T_c. (Note: the impurities in BaO_2 might be another reason for the lower T_c, J_c and trapped field observed for the NPP samples.)

3.5. Microstructure

The microstructures of the samples were investigated by optical microscopy and SEM, as shown in figure 8. It can be seen that concentration and distribution of the Y-211 phase inclusions in samples S1 (NPP) and S2 (CPP) at position 2c are very similar, and that the Y-211 particles are slightly smaller in sample S1. At the same time, it can be seen that sample S1 contains wider cracks and larger pores than sample S2, which may provide further explanation for the observed lower levitation force and lower trapped field in this sample due to the reduction in effective J_c, which is determined critically by the microstructure of the sample.

Overall, the superconducting properties of sample S1, fabricated from sintered raw oxides, are inferior to those of sample fabricated from pure Y-123 and Y-211, although the magnitude of the values of the critical parameters for practical applications are comparable to samples fabricated using commercial Y-123 and Y-211 precursor powders. It is known that the macroscopic superconducting properties, such as trapped field and levitation force, correlate closely with the local J_c and its distribution within the single grain. A low and varying J_c throughout the bulk microstructure, therefore, are possible explanations for the observed lower levitation force and trapped field. For the sample fabricated using sintered oxides, we can see from the comparison of microstructures in figure 8 that a combination of larger size pores and cracks leads directly to an unfavourable distribution of J_c. Therefore, the formation of larger pores and cracks in the NPP samples is almost certainly caused by incomplete sintering of the mixed precursor powder.

Figure 9 shows the x-ray diffraction (XRD) patterns of the samples fabricated by the NPP and CPP process after sintering at 890 °C for 10 h. Clearly, the NPP processed samples consit mainly of Y-123 and Y-211, which suggests that the majority of the metal oxide powders in these samples have reacted to form Y-123 and Y-211 phases after 10 h. However, the intensity of XRD peaks corresponding to the Y-123 phase are stronger and more pronounced in the samples processed using the CPP, which indicates that the conversion in the NPP powder from mixed oxides to Y-123 and Y-211 is not complete. This is, we suggest, the reason why the sample fabricated by the NPP has a lower T_c. This conclusion is supported further by the results of DTA of the precursor powders shown in figure 10. The weight of the NPP (which can be seen from the *y*-axis at the right side of figure 10) decreases rapidly between 925 °C and 950 °C (highlighted by a red circle) without apprent phase change, which suggests that unreacted oxides in the NPP precursor would continue to convert to the Y-123 and Y-211 phases during the continued heating process in the DTA measurement. This reaction would result in the release of gaseous O_2 as a product of the peritectic decomposition process, which, in turn, will generate additional pores in the sample microstructure. It can be seen from the DTA data that the conversion of the raw oxides can be completed by adjusting the sintering tempature for an appropriate sintering time. Finally, the NPP sintered oxide precursor undergoes the same peretictic reaction as the CPP samples, which suggests that an optimised heat treatment of the mixed raw oxide powder can form the Y-123 phase with good superconducting properties. This is the reason for the dwell segment at 930 °C for 10 h in the heating profile, although further research is required to further optimise these critical processing parameters for the raw oxide process.

In summary, the uncompleted conversion of the sintered raw oxides explains the observed lower and broader T_c and the presence of a larger pore inclusion and crack density, which, in turn, limits J_c and trapped field for the sample prepared from the NPP. However, the growth of a single grain is not affected adversely by the use of sintered oxides and the superconducting properties can be improved further via optimasing the sintering process.

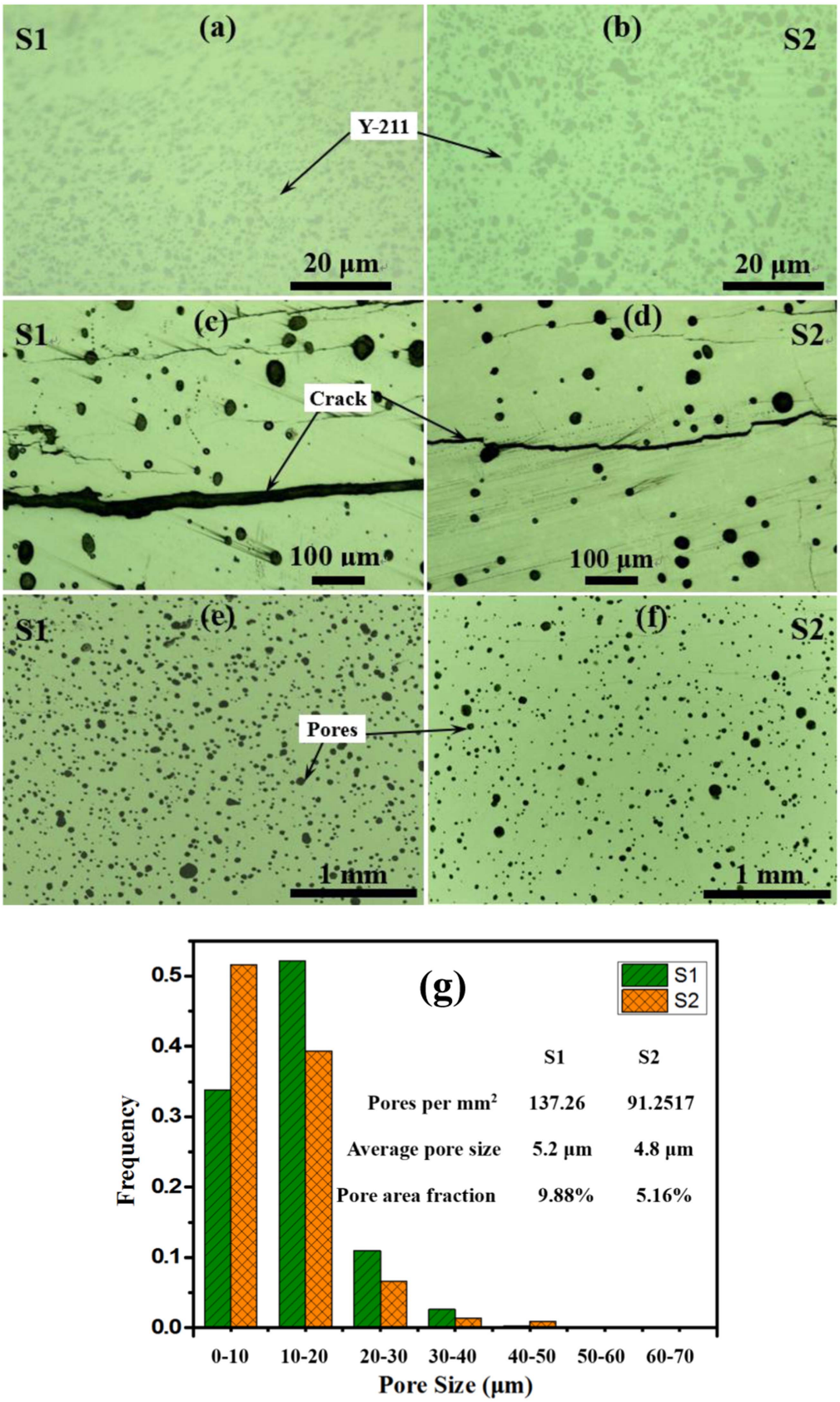

Figure 8. Microstructure of the YBCO samples. The Y-211 particle distribution in sample (a) S1 and (b) S2, cracks in sample (c) S1 and (d) S2, and pores in sample (e) S1 and (f) S2. (g) Histogram of pore size distribution in (e) and (f).

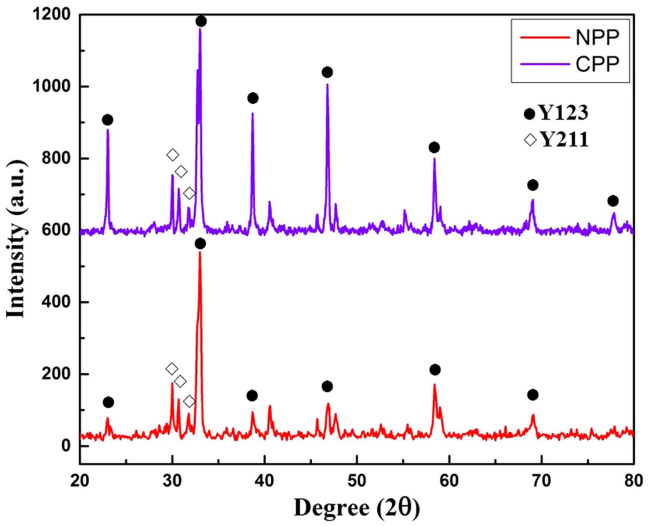

Figure 9. XRD patterns of NPP and CPP precursor powders.

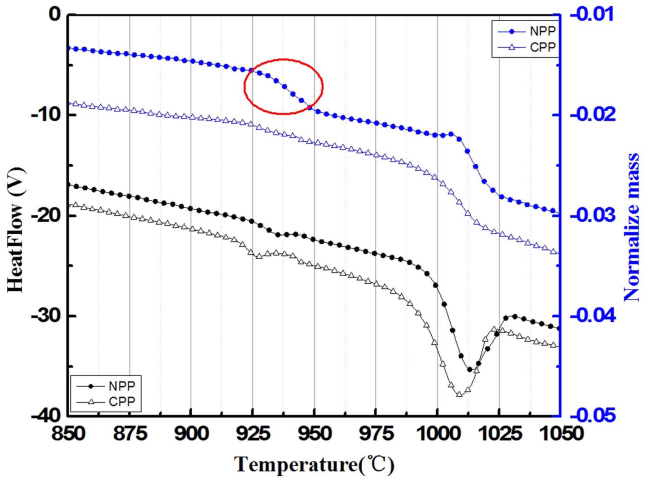

Figure 10. DTA results of NPP and CPP precursor powders.

4. Conclusions

We have demonstrated an effective technique for the fabrication of large, single grain YBCO using a sintered mixture of raw metal oxides, Y_2O_3, BaO_2 and CuO, as the precursor powder for the first time. This approach, therefore, constitutes a practical alternative to a mixture of commercial pure Y-123 and Y-211 powders used in conventional TSMG. Avoiding the pre-synthesis of Y-123 and Y-211 precursor phases results in a greatly simplified process, which leads, in turn, to savings in both time and cost. The average peak trapped magnetic field for single grain sample fabricated by the raw oxide precursor technique is 0.45 T for YBCO single grains of up to 20 mm in diameter. We believe that this technique has considerable potential for improving the applied properties of bulk YBCO superconductors with further optimization of this process.

Acknowledgments

This work was supported by the National Natural Science Foundation in China (No. 51572164), the China Scholarship Council (No. 201506875065), the Fundamental Research Funds for the Central Universities (No. GK201503023) and the Key Program of Science and Technology innovation team of Shaanxi Province (2014KTC-18). The authors acknowledge the financial support from the Engineering and Physical Sciences Research Council EP/P00962X/1. Additional data related to this publication are available at the University of Cambridge data repository (https://doi.org/10.17863/CAM.9899).

ORCID

Devendra Kumar Namburi https://orcid.org/0000-0003-3219-2708

References

[1] Wu M K, Ashburn J, Torng C, Hor P, Meng R, Gao L, Huang Z, Wang Y and Chu C W 1987 Superconductivity at 93 K in a new mixed-phase Y–Ba–Cu–O compound system at ambient pressure *Phys. Rev. Lett.* **58** 908–10

[2] Xu K-X, Wu D-J, Jiao Y L and Zheng M H 2016 A fully superconducting bearing system for flywheel applications *Supercond. Sci. Technol.* **29** 064001

[3] Werfel F N, Floegel-Delor U, Rothfeld R, Riedel T, Goebel B, Wippich D and Schirrmeister P 2013 Large-scale HTS bulks for magnetic application *Physica* C **484** 6–11

[4] Strasik M, Hull J R, Johnson P E, Mittleider J, McCrary K E, McIver C R and Day A C 2008 Performance of a conduction-cooled high-temperature superconducting bearing *Mater. Sci. Eng.* B **23** 034021

[5] Del-Valle N, Sanchez A, Navau C and Chen D-X 2011 Magnet guideways for superconducting maglevs: comparison between halbach-type and conventional arrangements of permanent magnets *J. Low Temp. Phys.* **162** 62

[6] Tomita M and Murakami M 2003 High-temperature superconductor bulk magnets that can trap magnetic fields of over 17 tesla at 29 K *Nature* **421** 517–20

[7] Durrell J H *et al* 2014 A trapped field of 17.6 T in melt-processed, bulk Gd–Ba–Cu–O reinforced with shrink-fit steel *Supercond. Sci. Technol.* **27** 082001

[8] Okajima N, Oura Y, Ohsaki H, Teshima H and Morita M 2013 Trapped flux and current density distributions of a 140 mm diameter large single-grain Gd–Ba–Cu–O bulk superconductor fabricated with RE compositional gradient method *Phys. Proc.* **45** 269–72

[9] Zhao W, Shi Y, Radušovská M, Dennis A R, Durrell J H, Diko P and Cardwell D A 2016 Comparison of the effects of platinum and CeO_2 on the properties of single grain, Sm–Ba–Cu–O bulk superconductors *Supercond. Sci. Technol.* **29** 125002

[10] Chen Y L, Chan H M, Harmer M P, Todt V R, Sengupta S and Shi D 1994 A new method for net-shape forming of large, single-domain $YBa_2Cu_3O_{6+x}$ *Physica* C **234** 232

[11] Namburi D K, Shi Y, Palmer K G, Dennis A R, Durrell J H and Cardwell D A 2016 An improved top seeded infiltration growth method for the fabrication of Y–Ba–Cu–O bulk superconductors *J. Eur. Ceram. Soc.* **36** 615–24

[12] Su X-Q, Yang W-M, Yang P-T, Zhang L-L and Abula Y 2017 A novel method to fabricate single domain YBCO bulk superconductors without any residual liquid phase by Y + 011 TSIG technique *J. Alloys Compd.* **692** 95

[13] Meng R L, Gao L, Gautier-Picard P, Ramirez D, Sun Y Y and Chu C W 1994 Growth and possible size limitation of quality single-grain $YBa_2Cu_3O_7$ *Physica* C **232** 337

[14] Meslin S, Iida K, Hari Babu N, Cardwell D A and Noudem J G 2006 The effect of Y-211 precursor particle size on the microstructure and properties of Y–Ba–Cu–O bulk superconductors fabricated by seeded infiltration and growth *Supercond. Sci. Technol.* **19** 711

[15] Shi Y, Namburi D K, Wang M, Durrell J, Dennis A, Cardwell D and Goyal A 2015 A reliable method for recycling (RE)–Ba–Cu–O (RE: Sm, Gd, Y) bulk superconductors *J. Am. Ceram. Soc.* **98** 2760

[16] Namburi D K, Shi Y, Palmer K G, Dennis A R, Durrell J H and Cardwell D A 2016 A novel, two-step top seeded infiltration and growth process for the fabrication of single grain, bulk (RE)BCO superconductors *Supercond. Sci. Technol.* **29** 095010

[17] Wang M, Yang W M, Wang M Z and Wang X J 2013 Effect of $Y_2Ba_4CuBiO_y$ nanoparticles doping on the levitation force of single-domain YBCO bulk superconductor by top-seeded infiltration process *J. Supercond. Nov. Magn.* **26** 3221–4

[18] Li G-Z, Yang W-M, Cheng X-F, Fan J and Guo X-D 2009 A modified TSIG technique for simplifying the fabrication process of single-domain GdBCO bulks with a new kind of liquid source *J. Mater. Sci.* **44** 6423

[19] Yang W M, Zhi X, Chen S L, Wang M, Li J W, Ma J and Chao X X 2014 Fabrication of single domain GdBCO bulk superconductors by a new modified TSIG technique *Physica* C **496** 1–4

[20] Guo Y-X, Yang W-M, Li J-W, Guo L-P, Chen L-P and Li Q 2015 Effects of vertical temperature gradient on the growth morphology and properties of single domain YBCO bulks fabricated by a new modified TSIG technique *Cryst. Growth Des.* **15** 1771

[21] Chen P-W, Chen I-G, Chen S-Y and Wu M-K 2011 The peak effect in bulk Y–Ba–Cu–O superconductor with CeO_2 doping by the infiltration growth method *Supercond. Sci. Technol.* **24** 085021

[22] Bean C P 1964 Magnetization of high-field superconductors *Rev. Mod. Phys.* **36** 31

[23] Yang W M and Wang M 2013 New method for introducing nanometer flux pinning centers into single domain YBCO bulk superconductors *Physica* C **493** 128–31

[24] Congreve J V J, Shi Y, Dennis A R, Durrell J H and Cardwell D A 2017 Improvements in the processing of large grain, bulk Y–Ba–Cu–O superconductors via the use of additional liquid phase *Supercond. Sci. Technol.* **30** 015017